

## DEVELOPMENT OF MICROSTRUCTURE DURING THE HOT PLASTIC DEFORMATION OF HIGH CLEAN STEELS FOR POWER PLANTS

### RAZVOJ MIKROSTRUKTURE MED VROČO PLASTIČNO DEFORMACIJO VISOKO ČISTEGA JEKLA ZA ENERGETSKE NAPRAVE

Kuskulic, Tomas<sup>1</sup>, Kvackaj, Tibor<sup>1</sup>, Fujda, M.<sup>1</sup>, Pokorný, I.<sup>1</sup>, Bacsó J.<sup>1</sup>, Molnarova, M.<sup>1</sup> Kocisko, R.<sup>1</sup>, Weiss, Michael<sup>2</sup>, Bevilaqua, Tomas<sup>2</sup>

<sup>1</sup> Technical university of Košice, Letna 9, 04200 Košice, Slovakia

<sup>2</sup> ZP-Podbrezova a.s., Kockaren 35, 97681 Podbrezova, Slovakia

Prejem rokopisa – received: 2007-09-28; sprejem za objavo – accepted for publication: 2008-01-11

The effect of the deformation and the deformation temperature on the primary austenite grain size, the recrystallisation and the mechanical properties of high clean steel STN 41 6537 (STN standard) were investigated. This steel grade is used for the forged rotors of steam turbines in power-generation facilities.

Key words: steel, power generation, forging, recrystallisation, mechanical properties

Raziskan je bil vpliv deformacije in deformacijske temperature na velikost avstenitnih zrn, rekristalizacijo in mehanske lastnosti zelo čistega jekla STN 416537 (STN standard). To jeklo se uporablja za kovane rotorje parnih turbin pri proizvodnji električne energije.

Ključne besede: jeklo, proizvodnja energije, kovanje, rekristalizacija, mehanske lastnosti

### 1 INTRODUCTION

The world is characterised by a constantly increasing population and a demand for improved living conditions. The industrialisation of a country depends strongly on the availability of electrical energy, which plays a key role in the rate of development<sup>1</sup>.

Modern high-pressure steam turbines operate under high working loads and at high temperatures. For this reason, much concern has been paid to the fatigue and creep behaviours of turbine materials. The rotor of a steam turbine also operates at high temperatures, and during complex stressing some cracks are likely to initiate. In addition to fatigue, creep damage plays an important role in rotor damage. Generally speaking, low-cycle fatigue uses up seventy percent of the life of the rotor, and creep accounts for the remaining thirty percent<sup>2</sup>. However, fatigue and creep always occur together, and the coupling of fatigue and creep must be considered in the lifetime prediction of a steam-turbine rotor<sup>3</sup>.

Much effort has been spent on developing a new, high-strength ferritic resistant steel, which would also be used for large components of fossil-fuel-fired power plants<sup>4</sup>. Because of the degradation during long-term service at elevated temperatures that causes changes in the microstructure<sup>5</sup>, an improvement in microstructural stability is a prerequisite for achieving excellent long-term creep strength. New steels have been widely used in modern fossil-fuel-fired power plants and in many investigations the correlations between the microstructure and the mechanical properties have been reported<sup>6</sup>.

The hot-working behaviour, in conjunction with the changes in the microstructure and the degradation during long-term creep deformation, is investigated and discussed in this article.

### 2 MATERIAL AND EXPERIMENTS

For the experiments a steel based on CrNiMoV was used; this is equivalent to STN 41 6537, with the chemical composition described in **Table 1**.

**Table 1:** Chemical composition  
**Tabela 1:** Kemična sestava

C	Mn	Si	P	S	Cr	Ni	Cu	Mo	V	Al	As	Sn	Sb	Ca	H	N	O
w/%																	
0.29	0.04	<0.01	0.003	0.003	1.57	2.84	0.010	0.39	0.11	0.004	11	8	<5	20	0.5	44	25

The experiments were designed to determine the influence of temperature and deformation on the austenite grain size. For the tests on the influence of the finish forging temperature and the final amount of deformation on the evolution of austenite grain size, the hot-working schedule in **Figure 1** was applied. The experimental samples of size (26 × 30 × 55) mm were heated under controlled conditions in air and cooled down to the first deformation temperature  $T_{\varepsilon 1} = 1100^{\circ}\text{C}$  in  $t_{1,\text{hold}} = 22$  s and then deformed for  $\varepsilon_1 = 50\%$ . The first plastic deformation was followed by holding the samples at the second deformation temperature  $T_{\varepsilon 2}$  in a chain conveyer furnace for  $t_{2,\text{hold}} = 80/100/120/150$  s. Afterwards, the forgings were cooled from  $T_{\varepsilon 1}$  to  $T_{\varepsilon 2} = (800/850/900/950)^{\circ}\text{C}$  and then submitted to a second plastic deformation  $\varepsilon_2 = (10/20/30/40/50/60)\%$  and finally quenched in a KOH water solution. Next the samples were ground and polished and annealed at 550 °C for 48 h. After annealing the continuous layer of scale was removed with fine grinding and the grain boundaries revealed with stringers of oxide particles. Finally, the specimens were etched in a water solution of picric acid with the addition of CuCl and the microstructure was investigated with optical microscopy. The size of the statically recrystallised austenite grains was assessed with a linear method as an average of 20 measurements. In cases of the absence of static recrystallization of the austenite the average corrected austenite grain diameter was calculated from equations based on an assessment of the average effective nucleation area.

$$d_{\gamma, \text{kor}} = \frac{2000}{Sv(\text{gb} + \text{db})} \quad (1)$$

$$\begin{aligned} Sv(\text{gb} + \text{db}) &= 1000 \cdot [0,429 \cdot (d_{\gamma,0}) + 1,571(d_{\gamma,\perp})] = \\ &= \frac{1000}{d_{\gamma,0}} \cdot \left[ 0,429 \cdot (1 - \varepsilon_0) + \frac{1,571}{(1 - \varepsilon_2)} \right] \end{aligned} \quad (2)$$

where:

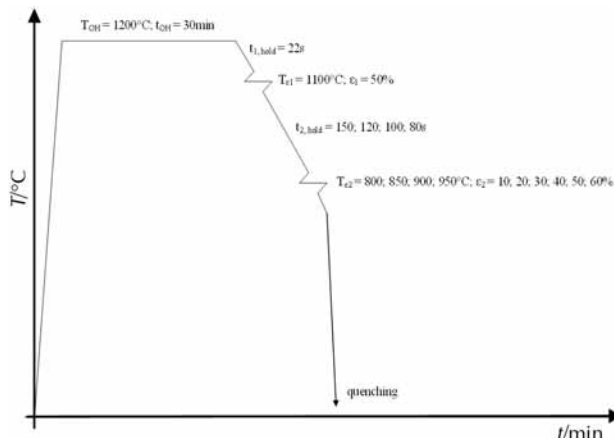


**Figure 1:** Temperature and deformation regime  
**Slika 1:** Režim temperature in deformacije

$d_{\gamma, \text{kor}}/\mu\text{m}$  is the corrected average diameter of an austenite grain,

$d_{\gamma,0}/\mu\text{m}$  is the recrystallised diameter of an austenite grain before the thermal area of the inhibited austenite recrystallisation.

$Sv(\text{gb} + \text{db})/(1/\text{mm})$  is the average effective nucleation area of the grain boundaries and deformation bands,

$Sv(\text{gb})$  is the effective nucleation area of the grain boundaries,

$Sv(\text{db})$  is the area of the deformation bands inside the austenite grains,

$\varepsilon_2/\%$  is the relative deformation.

In the case of static recrystallization of the austenite, the austenite grain diameter was deduced by applying the equation:

$$d_y = \frac{(1,68 \cdot d_{\text{kr}})}{(n \cdot zv)} \quad (3)$$

where:

$d_y/\mu\text{m}$  is the austenite grain diameter,

$d_{\text{kr}}/\text{mm}$  is the diameter of the circumference,

$n$  is the number of intersected grain boundaries,

$zv$  is the magnification.

The determined and deduced values for the grain size were then processed using non-linear numerical statistical methods and correlation equations for a description of the investigated dependences were generated.

### 3 RESULTS AND DISCUSSION

The influence of the final deformation and temperature on the austenite grain size is shown in **Figure 2 and 3**.

The obtained results show that with an increase in the amount of deformation  $\varepsilon_2$  above 10 % and deformation temperature  $T_{\varepsilon 2}$  above 850 °C the austenite grain diameter decreased from the original size  $d_{\gamma 1} = 43 \mu\text{m}$  after the first plastic deformation to  $d_{\gamma 2} = 7.7 \mu\text{m}$  for  $T_{\varepsilon 2}/\varepsilon_2 =$

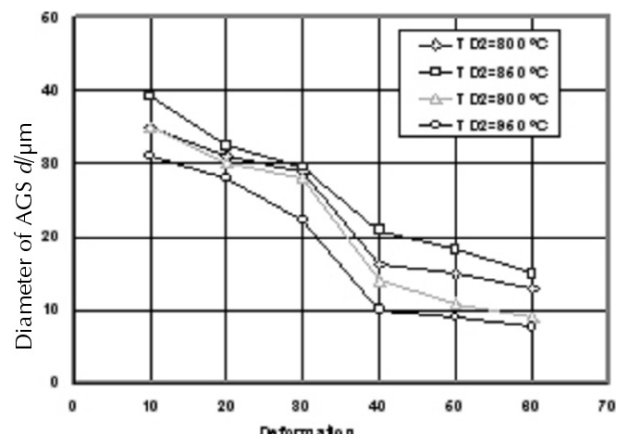


**Figure 2:** Dependence of AGS on deformation  
**Slika 2:** Ovisnost AGS (velikost avstjenitnih zrn) od deformacije

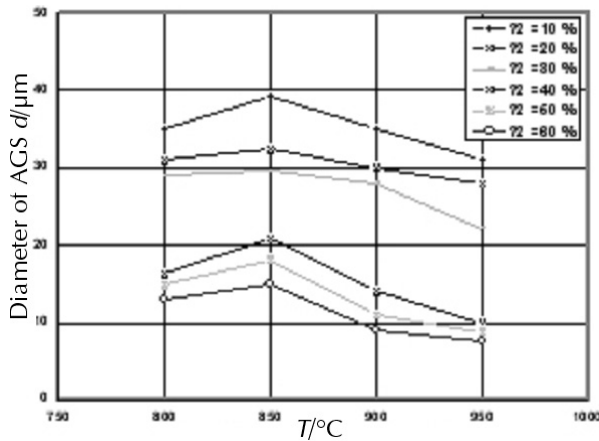


**Figure 3:** Dependence of AGS on deformation temperature  
**Slika 3:** Ovisnost AGS od temperature deformatije

950 °C/60 %, or to the size of  $d_{\gamma 2} = 15.0 \mu\text{m}$  for  $T_{\varepsilon 2}/\varepsilon_2 = 850 \text{ }^{\circ}\text{C}/60 \text{ %}$ .

- for  $\varepsilon_2/\% \in <10;30>$  and the investigated temperature  $T_{\varepsilon 2}/\text{°C} \in <800;950>$  the diameter of the austenite grain achieved coarse values of  $d_{\gamma 2}/\mu\text{m} \in <2.2;39.3>$ . For  $\varepsilon_2/\% \in <40;60>$  and  $T_{\varepsilon 2}/\text{°C} \in <800;950>$  the diameter of the austenite grains achieved bottom values of  $d_{\gamma 2} \in <7.7; 20.9> \mu\text{m}$ .

For an explanation of the occurrence of two areas of austenite grain size it was necessary to determine the share of static recrystallised austenite after the second deformation. The influence of the deformation  $\varepsilon_2$  and of the deformation temperature  $T_{\varepsilon 2}$  on the share of the static recrystallisation of austenite is shown in **Figures 4 and 5**.

- For the deformation  $\varepsilon_2/\% \in <10;30>$  and the temperature  $T_{\varepsilon 2}/\text{°C} \in <800;950>$  the share of statically recrystallised austenite was of  $X_{\text{SR}}/\% \in <0;20>$ .
- For the deformation  $\varepsilon_2/\% \in <40;60>$  and the temperatures  $T_{\varepsilon 2} = 800 \text{ }^{\circ}\text{C}$  and  $950 \text{ }^{\circ}\text{C}$  the share of statically recrystallised austenite was in the range of  $X_{\text{SR}}/\% \in <50;100>$  and it was classified as partly or completely recrystallised.

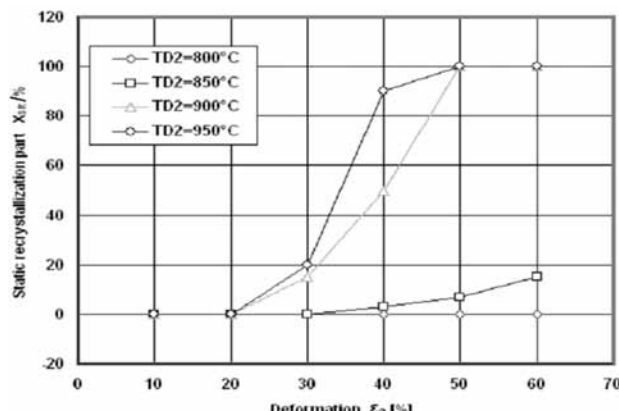


**Figure 4:** Dependence of  $X_{\text{SR}}$  on deformation  
**Slika 4:** Ovisnost  $X_{\text{SR}}$  (deleža rekristalizacije) od deformacije

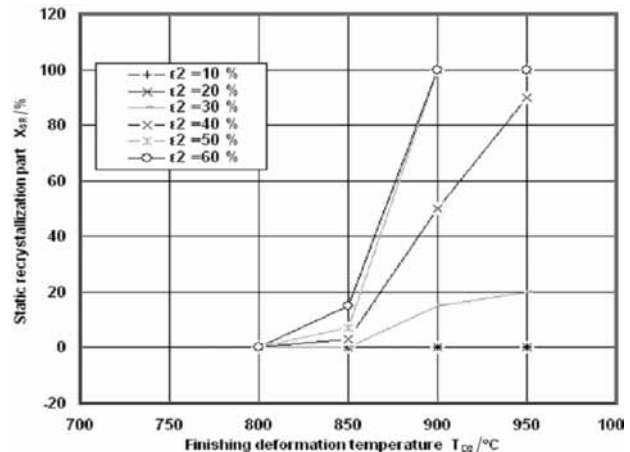


**Figure 5:** Dependence of  $X_{\text{SR}}$  on temperature  
**Slika 5:** Ovisnost  $X_{\text{SR}}$  od temperature

- For the deformation  $\varepsilon_2/\% \in <50;60>$  and the deformation temperatures  $T_{\varepsilon 2} = 900 \text{ }^{\circ}\text{C}$  and  $950 \text{ }^{\circ}\text{C}$  the share of statically recrystallised austenite was of  $X_{\text{SR}} = 100 \text{ %}$  and it was classified as completely recrystallised.
- For the deformation of  $\varepsilon_2 = 40 \text{ %}$  and the temperature of  $T_{\varepsilon 2} = 950 \text{ }^{\circ}\text{C}$  the share of statically recrystallised austenite was of  $X_{\text{SR}} = 90 \text{ %}$ , and it is also classified as completely recrystallised.

It can be concluded that the best conditions for attaining a completely statically recrystallised austenite are a deformation of  $\varepsilon_2 = 50$  and  $60 \text{ %}$  at  $T_{\varepsilon 2} = 900 \text{ }^{\circ}\text{C}$  and  $950 \text{ }^{\circ}\text{C}$ . In this case the size of the austenite grain is in the range  $d_{\gamma 2} = 7.7-11.0 \mu\text{m}$ .

Also, the static recrystallisation of austenite of ( $X_{\text{SR}} \geq 90 \text{ %}$ ) is achieved for a deformation of  $\varepsilon_2 = 40 \text{ %}$  and a temperature of  $T_{\varepsilon 2} = 950 \text{ }^{\circ}\text{C}$ ; however, the attained size of the austenite grain is  $d_{\gamma 2} = 10 \mu\text{m}$ .

The experimental numerical data were processed using linear and non-linear statistical methods, and the dependence of the final temperature, the amount of deformation and the austenite grain diameter were determined. Two equations were obtained for the dependence  $d_{\gamma 2} = f(\varepsilon_2; T_{\text{D}2})$ .

#### 1) Equation

$$d_{\gamma 2} = A0 \times T_{\text{D}2}^{A1} \times \varepsilon_2^{A2} \quad (4)$$

where:

$T_{\text{D}2}/\text{°C}$  is the second deformation temperature,

$\varepsilon_2/\%$  is the relative deformation,

$A0 = 2.54585 \times 10^7$

$A1 = -2.2021262$

$A2 = -0.697277$

A graphical comparison of the calculated and measured values is shown in **Figure 6**. For the deformation of  $\varepsilon_2 = 30 \text{ %}$  a strong deviation is found.

#### 2) Equation

$$d_{\gamma 2} = B0 \times \ln[1/(1-\varepsilon)]^{B1} \times Z^{B2} \quad (5)$$

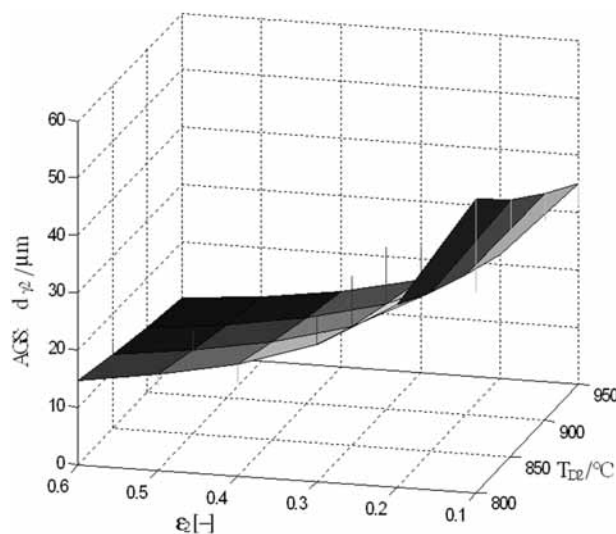


**Figure 6:** Comparaison of measurement and calculated values for equation

Slika 6: Primerjava meritev in izračunov z enačbo (4)

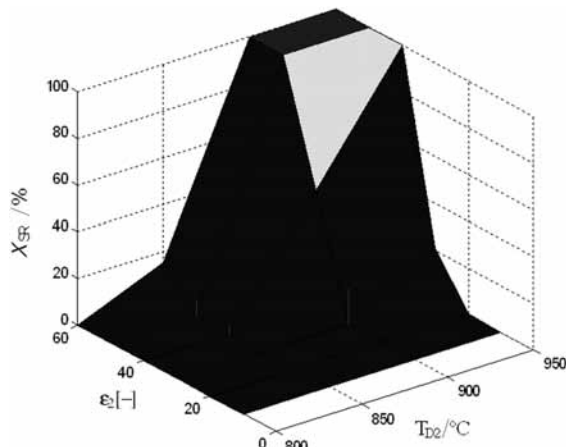


**Figure 7:** Comparaison of measurement and calculated values for equation

Slika 7: Primerjava meritev in izračunov z enačbo (6)

where:

$\epsilon/\%$  is the relative deformation,

$Z/s^{-1}$  is Zener-Holomon's parameter,

$B0 = 0.4913$

$B1 = -0.6347$

$B2 = 0.07653$

Equation (6) was deduced for describing the dependence share of the recrystallisation versus the extent of the deformation and the temperature

$$X_{SR} = 100 \cdot \left\{ 1 - e^{[a_1(\epsilon_2 - 0.1)^{a_2}(T_{D2} - 800)^{a_3}]} \right\} \quad (6)$$

where:

$X_{SR}/\%$  is the amount of statically recrystallised austenite,

$\epsilon_2/\%$  is the relative deformation,

$T_{D2} / ^\circ C$  is the second deformation temperature,

$a1 = -3.49 \cdot 10^{-22}$

$$a2 = 18.1048$$

$$a3 = 15.38$$

A graphical comparison of the calculated and measured values is shown in **Figure 7**.

#### 4 CONCLUSION

We performed experiments to investigate the effect of changes of the final deformation and deformation temperature on the austenite grain size and on the share of static austenite recrystallisation. From the results of these experiments the conditions necessary to design the technology for crankshaft smith forging were established:

the best conditions leading to a completely static recrystallisation of austenite ( $X_{SR} = 100 \%$ ) with forging are  $\epsilon_2 = 50$  and  $60 \%$  at  $T_{D2} = 900 \text{ } ^\circ C$  and  $950 \text{ } ^\circ C$ .

In these conditions an austenite grain size of  $d_{\gamma 2} = 7.7-11.0 \mu m$  is achieved,

- acceptable conditions leading to the static recrystallization of austenite ( $X_{SR} = 90 \%$ ) are  $\epsilon_2 = 40 \%$  at  $T_{D2} = 950 \text{ } ^\circ C$ , which ensure an austenite grain size of  $d_{\gamma 2} = 10 \mu m$ ;

- with the application of numerical statistical methods for the processing of experimental data, equations for the influence of temperature on the extent of the deformations on the size of the austenite grains were derived, together with the austenite static recrystallization.

#### Acknowledgements

The authors acknowledge the support given by the EUREKA E!3192 ENSTEEL.

#### 5 REFERENCES

<sup>1</sup> Feldmüller, A., Kern, T. U.: Design and materials for modern steam power plants an actual concept, In: PARSONS 2000 Advanced materials for 21<sup>st</sup> century turbines and power plant, 2000, Proceedings of the fifth international Charles Parsons turbine conference, 2000, 143-156

<sup>2</sup> Sedmak, A., Sedmak, S.: Critical crack assessment procedure for high pressure steam turbine rotors, In: Fatigue Fract Eng Mater Struct 18 (1995), 23-24

<sup>3</sup> Jing JianPing, Meng Guang, Sun Yi, Xia SongBo: An effective continuum damage mechanics model for creep-fatigue life assessment of a steam turbine rotor: International Journal of Pressure Vessels and Piping 80 (2003), 389-396

<sup>4</sup> Abe, F., Igarashi, M., Fujisuna, N., Kimura, K., Muneki S.: Materials for advanced power engineering, In: Proceedings of sixth liege conference, Materials for advanced power engineering, Ibid 1, 1998, 259

<sup>5</sup> Kimura, K., Kushima, H., Abe, F., Yagi, K., Irie, H.: Assessment of creep strength properties of 9 to 12 % steels from a viewpoint of inherent creep strength, In: Advances in turbine materials, design and manufacturing, Proceedings of fourth international Charles Parsons turbine conference, 1997, 257-269

<sup>6</sup> Masuyama, F., Nishimura, N.: Strength of materials, In: The Japan Institute Metals, Advanced materials and technologies 2 (1994), 204